Sensors & Diagnostics

PAPER

View Article Online
View Journal | View Issue

Cite this: *Sens. Diagn.*, 2023, **2**, 1638

Integrated sampling-and-sensing using microdialysis and biosensing by particle motion for continuous cortisol monitoring†

Laura van Smeden, [ac] Arthur M. de Jong [bc] and Menno W. J. Prins *[abcd]

Microdialysis catheters are small probes that allow sampling from biological systems and human subjects with minimal perturbation. Traditionally, microdialysis samples are collected in vials, transported to a laboratory, and analysed with typical turnaround times of hours to days. To realize a continuous sampling-and-sensing methodology with minimal time delay, we studied the integration of microdialysis sampling with a sensor for continuous biomolecular monitoring based on Biosensing by Particle Motion (BPM). A microfluidic flow cell was designed with a volume of 12 μl in order to be compatible with flowrates of microdialysis sampling. The analyte recovery and the time characteristics of the sampling-and-sensing system were studied using a food colorant in buffer and using cortisol in buffer and in blood plasma. Concentration step functions were applied, and the system response was measured using optical absorption and a continuous BPM cortisol sensor. The cortisol recovery was around 80% for a 30 mm microdialysis membrane with a 20 kDa molecular weight cut-off and a flowrate of 2 μl min^{-1}. The concentration-time data could be fitted with a transport delay time and single-exponential relaxation curves. The total delay time of the sampling-and-sensing methodology was about 15 minutes. Continuous sampling-and-sensing was demonstrated over a period of 5 hours. These results represent an important step toward integrated sampling-and-sensing for the continuous monitoring of a wide variety of low-concentration biomolecular substances for applications in biological and biomedical research.

Received 18th July 2023,
Accepted 8th October 2023

DOI: 10.1039/d3sd00185g

rsc.li/sensors

Introduction

Microdialysis is an analyte collection method that was first used to quantify dopamine levels in neural tissue.[1–3] It is now broadly applied in life-science research, biomedical research and in clinical settings for taking samples from the brain, skin, organs, and blood vessels.[4–9] Microdialysis probes contain a semi-permeable membrane that allows diffusive exchange of molecules between a biological medium and a dialysis fluid. Analytes can be small molecules or proteins, depending on the molecular weight cut-off (MWCO) of the membrane. A critical parameter in microdialysis sampling is the flow speed of the perfusion fluid, typically around a microliter per minute, because it determines the sampling time and the recovery, *i.e.* the concentration of analyte in the collected dialysis fluid with respect to the concentration of analyte in the biological medium.

The continuous nature of microdialysis makes it a highly interesting sampling methodology for integration with continuous sensing methodologies, in order to enable measurements of concentration-time profiles in biological systems. The measurement methods need to be compatible with the low flowrates of microdialysis and operate in a continuous manner so that analytical data can become available with a minimal time delay.[10] The integration of microdialysis sampling with continuous sensing has already been demonstrated for the monitoring of metabolites and neurotransmitters at millimolar concentrations, using electrochemical[11,12] and optical[10,13] sensing techniques, including studies with patients.[14] An important next step will be to enable the continuous monitoring of analytes with much lower concentrations, which requires the integration of microdialysis with sensors that have high sensitivities.

An interesting analyte for continuous monitoring is cortisol, a steroid stress hormone that affects almost all tissues and organs in the body and that has concentrations that fluctuate over time in the (sub)micromolar range.

[a] *Department of Biomedical Engineering, Eindhoven University of Technology, 5600 MB Eindhoven, The Netherlands. E-mail: m.w.j.prins@tue.nl*
[b] *Department of Applied Physics, Eindhoven University of Technology, 5600 MB Eindhoven, The Netherlands*
[c] *Institute for Complex Molecular Systems (ICMS), Eindhoven University of Technology, 5600 MB Eindhoven, The Netherlands*
[d] *Helia Biomonitoring, De Lismortel 31, 5612 AR Eindhoven, The Netherlands*

† Electronic supplementary information (ESI) available: Calibration curves, droplet evaporation, membrane permeability, effect of albumin, additional demonstrations of the integrated setup, and supporting tables. See DOI: **https://doi.org/10.1039/d3sd00185g**

Microdialysis has previously been applied to sample cortisol from saliva and serum[15–17] and from a variety of intravenous and subcutaneous sampling sites.[18,19] We recently reported the development of a reversible continuous cortisol sensor for the monitoring of elevated cortisol levels, tested with samples taken from buffer and blood plasma by microdialysis.[20] In this work, we report a study of the development of an integrated sampling-and-sensing system for the continuous monitoring of cortisol, where a microdialysis catheter was directly connected to a continuous cortisol sensor based on Biosensing by Particle Motion (BPM).[21–23] The dynamic properties of the integrated system were studied using a dye that was optically imaged and using cortisol that was measured by the BPM sensor. The measured concentration-time data could be fitted with an initial transport time and subsequent single-exponential relaxation curves. Continuous sampling-and-sensing was demonstrated for several hours with multiple applied concentration steps. Finally, we discuss the implications of these results for the development of continuous sampling-and-sensing systems that target the continuous monitoring of low-concentration substances using microdialysis.

Results and discussion

Continuous microdialysis with continuous sensing was experimentally studied using the system as sketched in Fig. 1. A perfusing fluid (the perfusate) was pumped *via* the inlet tubing into a microdialysis probe, which was placed in a container (the sampling site) containing buffer or blood

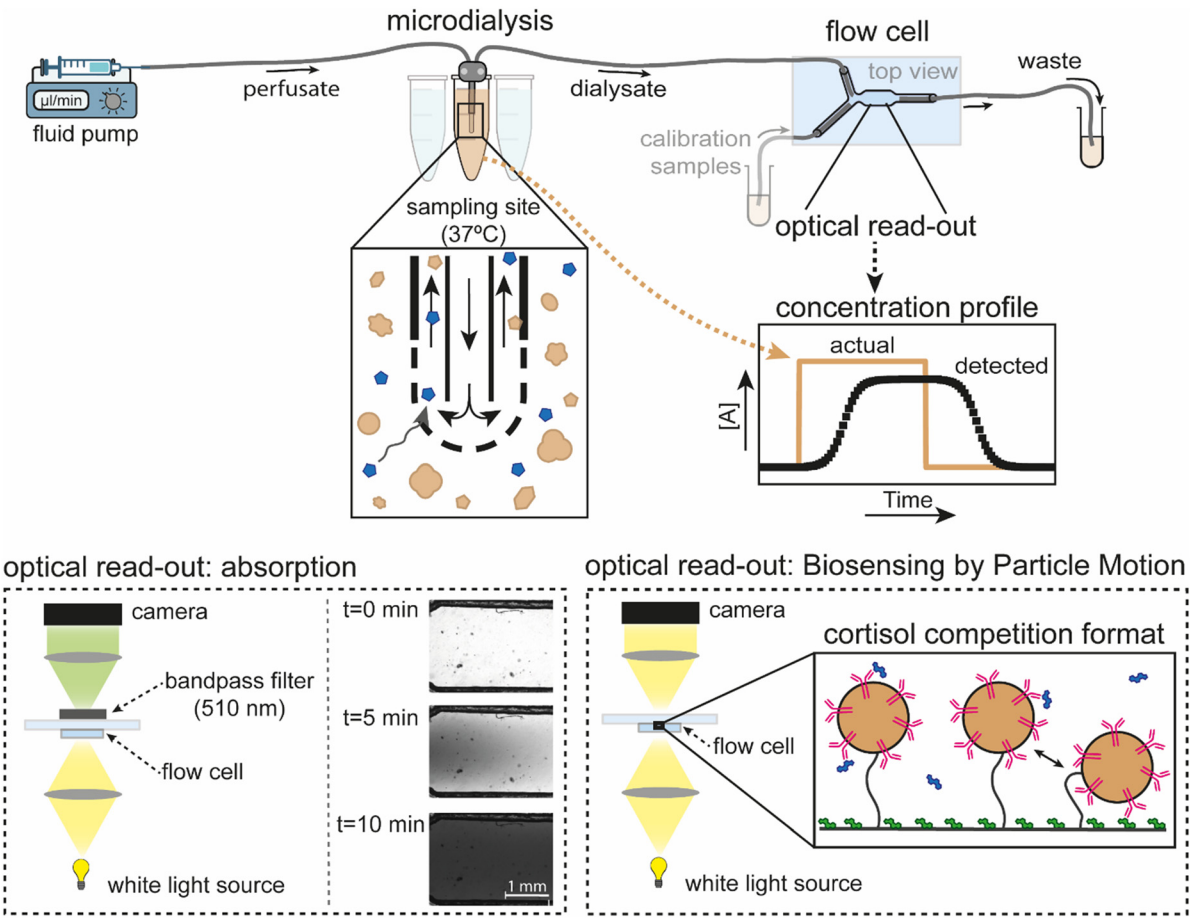

Fig. 1 Schematic of the experimental setup to study integrated continuous sampling-and-sensing using microdialysis and Biosensing by Particle Motion (BPM). The outlet of a microdialysis probe was connected to a flow cell with a chamber volume of 12 μl, wherein analyte concentrations [A] were measured by either optical absorption (left bottom) or by BPM (right bottom). The dialysate from the microdialysis probe was also collected for offline UV-vis spectroscopic analysis (not shown). Read-out *via* absorption was used for studies of fluid transport in the system, using the red food-colour dye azorubine. The azorubine concentration was measured using a microscope setup with 510 nm bandpass filter and 2.5× magnification, giving an overview of nearly the entire measurement chamber. Read-out *via* BPM was used for biosensing studies, including the dynamics of fluid transport and affinity reaction at the sensing surface. BPM is based on tracking the motion of biofunctionalized particles on a biofunctionalized sensing surface, using a microscope setup with 10× magnification, with the field-of-view in the middle of the measurement chamber. For continuous cortisol monitoring (cortisol depicted in blue), the particles were functionalized with anti-cortisol antibodies (pink) and the sensing surface with cortisol-analogue molecules (green).[20] The microdialysis probe was exposed to concentration step-functions by transferring the probe between different sample containers. Measured concentration-time profiles were compared to the applied concentration step-functions.

plasma as the medium, which was kept at body temperature (37 °C). The outlet tube of the microdialysis probe (with the dialysate) was connected to a flow cell for optical read-out using absorption measurements (see sketch in bottom left) or Biosensing by Particle Motion (BPM sensor, see bottom right). Alternatively, the dialysate was collected from the microdialysis outlet tube and analysed using UV-vis spectroscopy (not shown). These experiments were used (1) to quantify the recovery properties of the microdialysis probe for different flowrates, membrane lengths, and medium compositions, (2) to study the time characteristics of fluid transport in the integrated system with microdialysis probe and flow cell, and (3) to study the time characteristics of the total sampling-and-sensing system with microdialysis and BPM. Analyte transport was studied in the system using widefield absorption microscopy of an azorubine dye, for visualization and quantification with spatial and temporal resolution. Microscopy was also used for tracking the mobility of micrometer sized particles in order to continuously monitor the cortisol concentration using a BPM sensor.[20,23,24]

Cortisol recovery by the microdialysis probe

The recovery parameter characterizes the efficiency of analyte extraction by microdialysis, quantified as the ratio between the concentration of the analyte in the dialysate and the concentration of the analyte at the sampling site:[20,25] $\text{Recovery} = \frac{C_{\text{dialysate}}}{C_{\text{sample}}} \times 100\%$. Factors that influence the recovery are the flowrate (Q, with unit volume per time, typically µl min^{-1}) and the total area of the semipermeable membrane (A, with unit area, typically mm^2), which both appear in Jacobson's equation:[26] $\text{Recovery} = \frac{C_{\text{dialysate}}}{C_{\text{sample}}} = 1 - \exp\left(\frac{-K_0 \cdot A}{Q}\right)$, with K_0 the permeability coefficient or mass transfer coefficient (with unit velocity, typically µm s^{-1}).[3] Retro-dialysis is an alternative method to quantify recovery, where the perfusate contains the analyte and the medium does not, so a loss of analyte into the medium is studied; correspondingly the recovery is defined as: $\text{Recovery} = \left(1 - \frac{C_{\text{dialysate}}}{C_{\text{perfusate}}}\right) \times 100\%$.

Fig. 2 shows cortisol recovery data for a commercial microdialysis probe with a semipermeable membrane having 20 kD molecular-weight cut-off (MWCO), with a membrane length of 4 mm or 30 mm, using PBS as perfusate. The probe was inserted into PBS solutions with different cortisol concentrations, dialysate samples were collected at the outlet of the microdialysis tube, and the cortisol concentration in the dialysate samples was quantified using UV-vis spectroscopy. The UV-vis calibration curve is shown in Fig. S1,† demonstrating that the absorbance at 247 nm depends linearly on cortisol concentration in PBS, for concentrations between 7 and 600 µM. Water evaporation during sample collection resulted in increases of the cortisol concentration, especially for the lowest flowrate, which the data was corrected for (see ESI† section 2).

Fig. 2A shows the recovery for cortisol concentrations of 50–200 µM and three different flowrates. The recovery does not depend on the concentration and shows recovery values

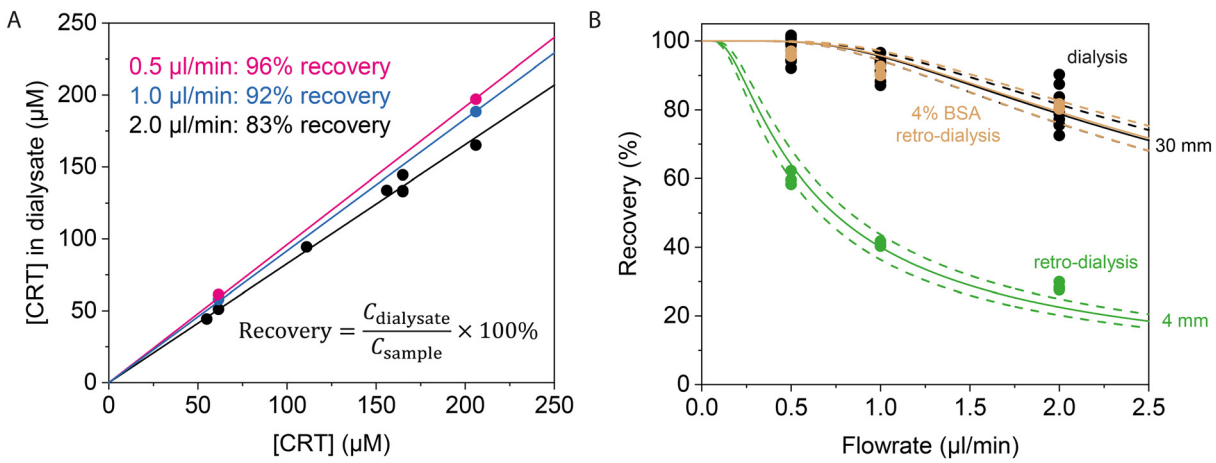

Fig. 2 Cortisol recovery studied for different cortisol (CRT) concentrations (50 to 200 µM) and perfusion flowrates, quantified for a commercial microdialysis probe with a semipermeable membrane having 20 kD molecular-weight cut-off (MWCO), with a membrane length of 4 mm or 30 mm, using PBS as perfusate. A) Cortisol recovery is quantified by the slope of the linear fit, with on the x-axis the [CRT] in the container and on the y-axis the [CRT] in the dialysate, studied for three flowrates: 2 µl min^{-1} (black), 1 µl min^{-1} (blue), and 0.5 µl min^{-1} (pink). A membrane length of 30 mm was used. B) Dependency of recovery on flowrate and membrane length (4 mm in green, 30 mm in black and brown) for [CRT] of 50–200 µM. Green and black datapoints were obtained by sampling from PBS and brown datapoints were sampled from 4% BSA in PBS. The black datapoints correspond to the data as presented in panel A. Datapoints are fitted with the Jacobson[26] equation $R = 1 - \exp\left(-\frac{K_0 \cdot A}{Q}\right)$; the dashed lines indicate the 95% confidence interval. The obtained (K_0·A)-values are 0.5 ± 0.1 µl min^{-1} for the 4 mm membrane and 3.1 ± 0.1 µl min^{-1} for the 30 mm membrane. Retro-dialysis with a medium of 4% BSA in PBS (brown) gives a (K_0·A)-value of 3.2 ± 0.1 µl min^{-1}.

of ~83 ± 1% for a flowrate of 2 μl min^{-1}, 92 ± 1% for 1 μl min^{-1}, and 96 ± 1% for 0.5 μl min^{-1}. Fig. 2B shows recovery data as a function of flowrate, for dialysis and retro-dialysis experiments. The cortisol recovery for 4 and 30 mm membrane lengths could be fitted with Jacobson's equation, giving values of the $K_0 \cdot A$ product of 0.5 ± 0.1 and 3.1 ± 0.1 μl min^{-1}, respectively. Based on the estimated membrane areas of 6.7 mm^2 and 48 mm^2 for the 4 and 30 mm membranes (using a probe radius of 0.25 mm), respectively, a permeability coefficient K_0 of about 1.2 μm s^{-1} was determined.

The effect of plasma proteins on the recovery was investigated with dialysis and retro-dialysis, using PBS solution with 4% BSA. BSA is a bovine plasma protein with a molecular weight of 66 kDa that does not pass the semipermeable membrane with 20-kDa MWCO, as confirmed in Fig. S3.† Dialysis and retro-dialysis sampling from the 4% BSA solution resulted a ~21 ± 4% decrease in the collected sample weight (see ESI† section 4 and Fig. S4), which can be attributed to the osmotic pressure due to the high protein concentration in the medium.

The recovery for sampling from 4% BSA as obtained with retro-dialysis (~80, 91, and 96%) is comparable with dialysis recoveries from buffer (~83, 92, and 96%) (Fig. 2B). However, dialysis from 4% BSA resulted in lower recoveries (Fig. S5C†). This may be attributed to binding of cortisol to BSA, which would decrease the free cortisol concentration in solution (see ESI† section 5).[27] Based on the retro-dialysis data, it can be concluded that the transport through the membrane only depends on the K_0, A and Q, and is not influenced by the presence of BSA proteins in the medium.

Transport properties of the integrated microdialysis-flow cell system studied using azorubine and cortisol

The analyte transport properties of the integrated system with microdialysis probe and connected flow cell (see Fig. 1) were investigated using azorubine and cortisol as analytes. Azorubine and cortisol are small molecules with similar molecular weights (502 Da and 362 Da, respectively) and diffusivities. Azorubine is a red colorant that is easily detected using absorption microscopy. The concentration of azorubine in the flow cell can be determined from the adsorption of light at 510 nm (ESI† section 6 and Fig. S6), allowing the study of sample transport (advection and diffusion) with a data frequency of 1 Hz.

The left-bottom panel in Fig. 1 shows microscopy images of the entire measurement chamber in the flow cell, during the first 10 minutes after a concentration step from 0 to 0.96 mM azorubine at the sampling site, with a perfusion flowrate of 2 μl min^{-1}. The image after 5 minutes shows concentration differences, with higher concentrations in the center and lower concentrations at the sides. Fig. 3A shows azorubine concentration-time profiles measured in different regions of interest (ROIs) in the flow cell. All measured curves show a behaviour that is close to a single-exponential relaxation function (with characteristic relaxation time τ) after a delay

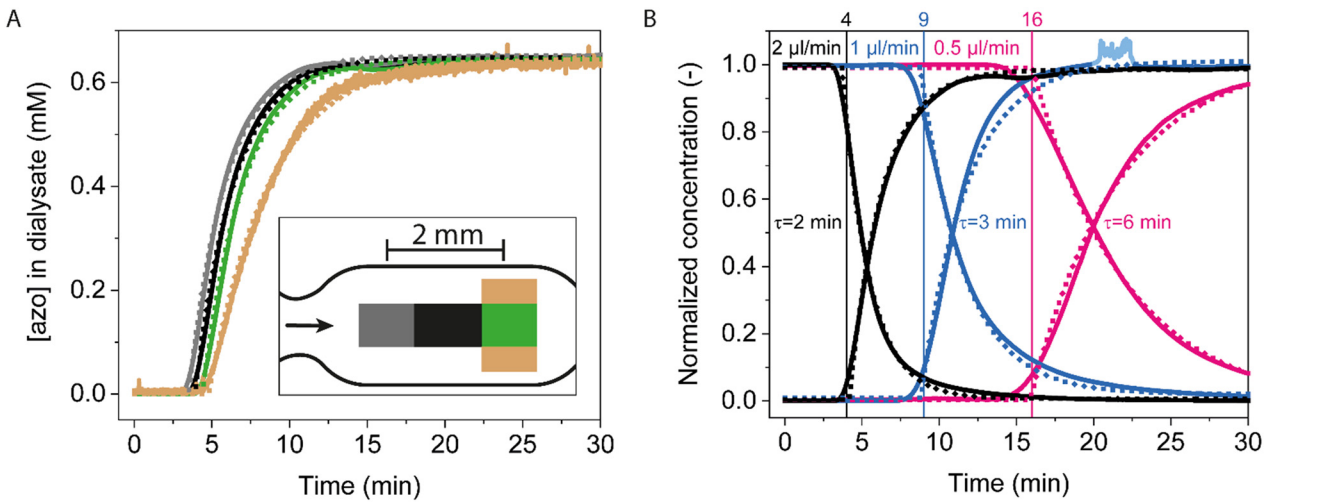

Fig. 3 Analyte transport in the integrated system, using azorubine as analyte, and sampling with a microdialysis probe with 30 mm membrane length and with PBS as perfusate. A) Optical absorption microscopy images were taken in various regions in the measurement chamber in the flow cell, see the inset (see Fig. S8† for more details). The perfusion flowrate was 2 μl min^{-1} and azorubine was sampled from 0.96 mM azorubine in PBS. The resulting concentration measurements are indicated as continuous lines and fits as dotted lines. The fits represent single-exponential relaxation curves, with a characteristic relaxation time τ, time-shifted with a delay time t_0. The delay time t_0 of the grey, black, and green fits differ by ~1 minute and corresponds to the time it takes to transport the sample over a 2 mm distance in the flow cell. B) Concentration-time profiles in the center of the measurement chamber, for step increases and step decreases of azorubine concentration ([azo] in sample container ranged from 0 to 1.92 mM), as a function of the applied perfusion flowrate: 2 (black), 1 (blue) and 0.5 (pink) μl min^{-1}. Continuous lines indicate measurements and dotted lines indicate single-exponential fits. The vertical lines indicate the t_0-values and the fitted τ-values are provided next to the graphs. The values per fit are provided in Tables S1 and S2.†

time t_0. The delay time is interpreted as the advective transport time that depends on the outlet volume of the microdialysis probe (~7 μl for the microdialysis probe plus its outlet tubing), the position in the flow cell relative to the flow cell inlet, and the flowrate. The delay times increase for the ROIs from left to right, caused by the longer travelling distance in the flow cell. The characteristic relaxation time τ is interpreted as the time required to homogenize the azorubine concentration in the system, by advection and diffusion in the microdialysis probe, the outlet tube and the flow cell. The brown curve shows the longest relaxation time, which we attribute to the higher hydrodynamic drag near the edges of the flow cell. Fig. 3B shows concentration-time profiles for different flowrates. The data show how the delay times and the relaxation times depend on the flowrate, with lower flowrates requiring longer times to replace and homogenize the fluid in the tubes and in the flow cell.

Fig. 4 shows concentration-time profiles for sequences of applied step functions, using solutions with azorubine and cortisol at a flowrate of 2 μl min^{-1}. The azorubine recovery values are similar to the cortisol recovery measured in Fig. 2. Fig. 4B shows the response curves superimposed to compare the time scales. The fits give an average t_0 value of 3.5 ± 0.4 min (n = 6) and τ = 2.3 ± 0.2 min. This gives $\Delta t_{95\%} = t_0 + \tau_{95\%} = t_0 + 3\tau$ = 10.4 ± 1.0 min for the total delay time to reach 95% of the concentration change.

Fig. 4C shows the response to a series of cortisol step functions measured at the outlet tube of the microdialysis probe. Dialysis samples were collected every 5 min and the cortisol concentration was determined offline using UV-vis spectroscopy, as in the experiment of Fig. 2. The data in Fig. 4C show the reproducibility of repeated sampling from solutions with varying cortisol concentrations. Fig. 4D shows the initial time-dependent response. By fitting the response, we find that t_0 is 3.4 ± 0.3 min and τ is 3.0 ± 0.3 min. However, due to the 5 min cortisol collection times, these numbers indicate upper boundaries rather than accurate estimations of the time values of the microdialysis probe.

Continuous sampling-and-sensing of cortisol using microdialysis and BPM

Fig. 5 shows the time-dependent response of the continuous sampling-and-sensing system using microdialysis and the cortisol BPM sensor. Fig. 5A shows the measurement setup where the microdialysis probe is connected to the flow cell, with the read-out of the cortisol BPM sensor in the central region of the measurement chamber. The flow cell has an extra input channel for the supply of calibration samples. Fig. 5B shows the applied concentrations and the measured bound fraction BPM signal as a function of time. The bound fraction is expressed as the temporal fraction of particles being in bound states.[23,24] The measured calibration data are used to establish a calibration curve that relates the BPM signal to the concentration (Fig. 5C, left panel; calibration curve for switching activity signal is shown in Fig. S9A and B†). The calibration curve is established for cortisol concentrations in the range between 0.4 and 30 μM, with an EC50 value of ~2 μM. Using the calibration curve, the subsequently measured bound fraction data ($t > 0$ in Fig. 5B) can be translated to apparent concentration values, as shown in the right panel of Fig. 5C.

Fig. 5D shows the responses to concentration changes corresponding to the six shaded areas in Fig. 5C, including fits of single-exponential relaxation curves. The fits for buffer indicate an average delay time t_0 of 4.1 ± 0.6 min and an average characteristic relaxation time τ of 3.0 ± 0.8 min. The t_0 values of cortisol sensing with BPM (Fig. 5D) and azorubine sensing by optical absorption (Fig. 3B) are similar, which indicates that t_0 is dominated by the transport phenomena that the two experiments have in common (transport through the microdialysis probe, the tubing, and the bulk of the flow cell) rather than transport differences between the two experiments (BPM sensing is a surface-sensitive measurement technique, while absorption measurements are sensitive to analyte in the bulk solution). The τ value is larger for cortisol sensing by BPM compared to azorubine sensing by optical absorption, which may be attributed to the slower intrinsic response of the cortisol BPM sensor compared to the optical absorption measurement. The time values give $\Delta t_{95\%} = t_0 + \tau_{95\%} = t_0 + 3\tau \cong 13 \pm 3$ min for the total time delay to reach 95% of the concentration change. Thus, the measurement series in Fig. 5 demonstrate that an integrated sampling-and-sensing system consisting of a microdialysis probe and a BPM flow-cell biosensor, enables continuous cortisol monitoring over a timespan of ~5 hours, with delay times and response times on timescales of several minutes.

Conclusions

We have developed an integrated sampling-and-sensing system for continuous biomolecular monitoring, based on microdialysis sampling and a flow cell biosensor. The recovery and the transport properties of a commercial microdialysis probe (CMA/20) were quantified and the time response of the integrated sampling-and-sensing system was studied using azorubine and cortisol as analytes.

The cortisol recovery of the microdialysis probe was characterized (~83% for 2 μl min^{-1}) and showed a flowrate dependency according to the Jacobson equation with a permeability coefficient of ~1.2 μm s^{-1}. The time response of the sampling-and-sensing system was characterized by a delay time and a single-exponential relaxation curve. The delay time is caused by advective transport through the microdialysis probe, the tubing, and the flow cell. The single-exponential relaxation behaviour relates to the homogenization of analyte concentration in the microdialysis probe, tubing, and the flow cell, together with the intrinsic response time of the analyte sensing method. At a flowrate of 2 μl min^{-1}, the integrated sampling-and-sensing system showed a total time delay of about 13 min to reach 95% of

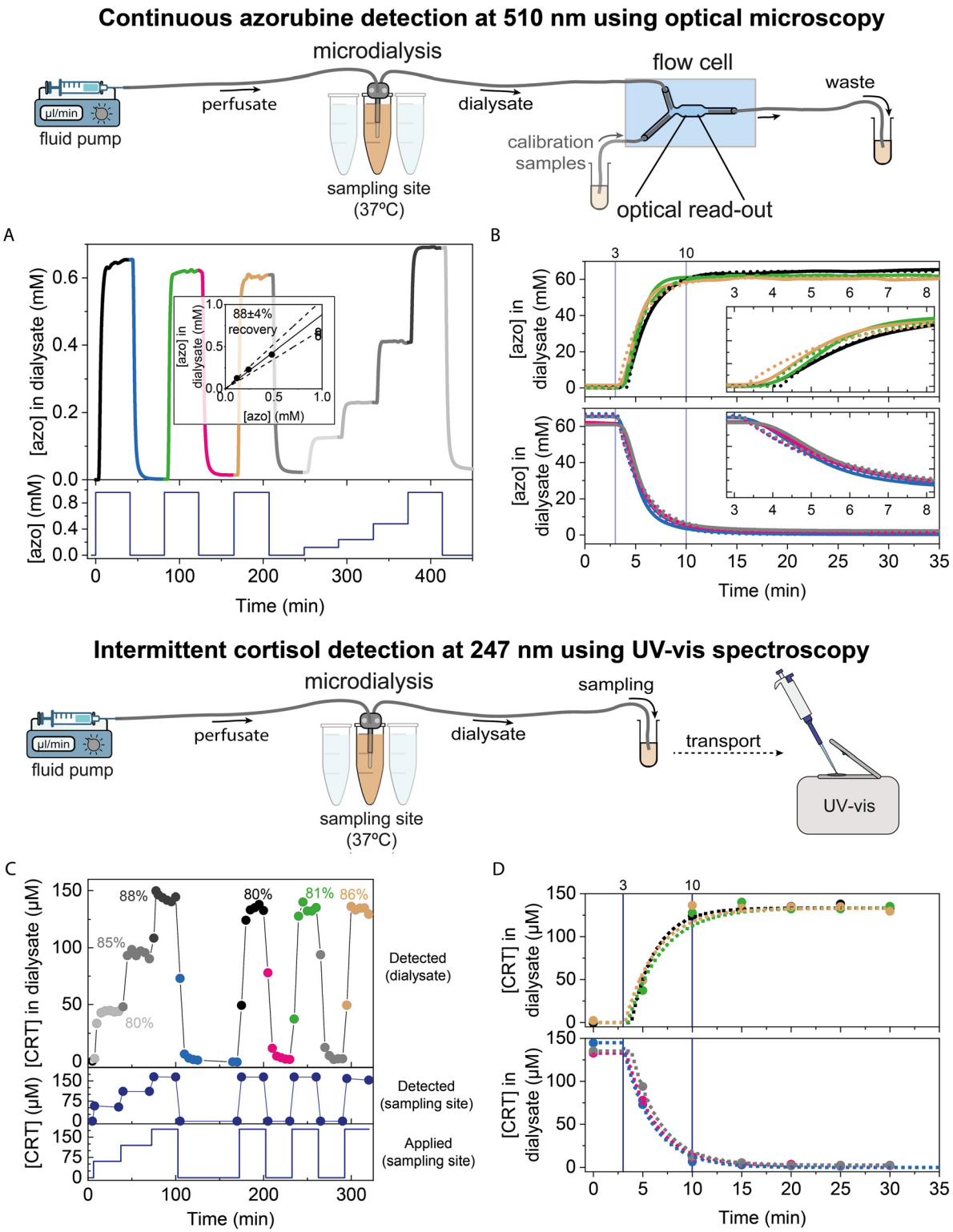

Fig. 4 Transport properties of the microdialysis system for series of applied concentration step functions, for azorubine and cortisol, using a microdialysis probe with 30 mm membrane length and a flowrate of 2 µl min^{-1} of PBS buffer. A) Azorubine concentration measured in the flow cell for a series of step functions. The highest concentration azorubine [azo] is 0.96 mM. The inset shows an azorubine recovery of 88 ± 4%; dashed lines indicate the 95% confidence interval. B) Superimposed representation of selected curves of panel A, showing that changes of signal are detectable after 3 minutes. Roughly 10 minutes are required to reach 95% of the signal change ($t_0 + \tau_{95\%} = t_0 + 3{\cdot}\tau$). Dotted lines indicate the single-exponential fits; the t_0- and τ-values are provided in Table S3.† C) Cortisol concentration ([CRT]) measured in dialysate using UV-vis spectroscopy. Samples with a volume of 10 µl were collected from the outlet of the microdialysis probe, each sample collected over a period of 5 min, as in the experiments of Fig. 2. D) Superimposed representation of selected curves of panel C, showing that changes of signal are detectable after 5 minutes. Roughly 10 minutes are required to reach 95% of the signal change. Dotted lines are guides to the eye, obtained *via* exponential fitting, see Table S4† for details.

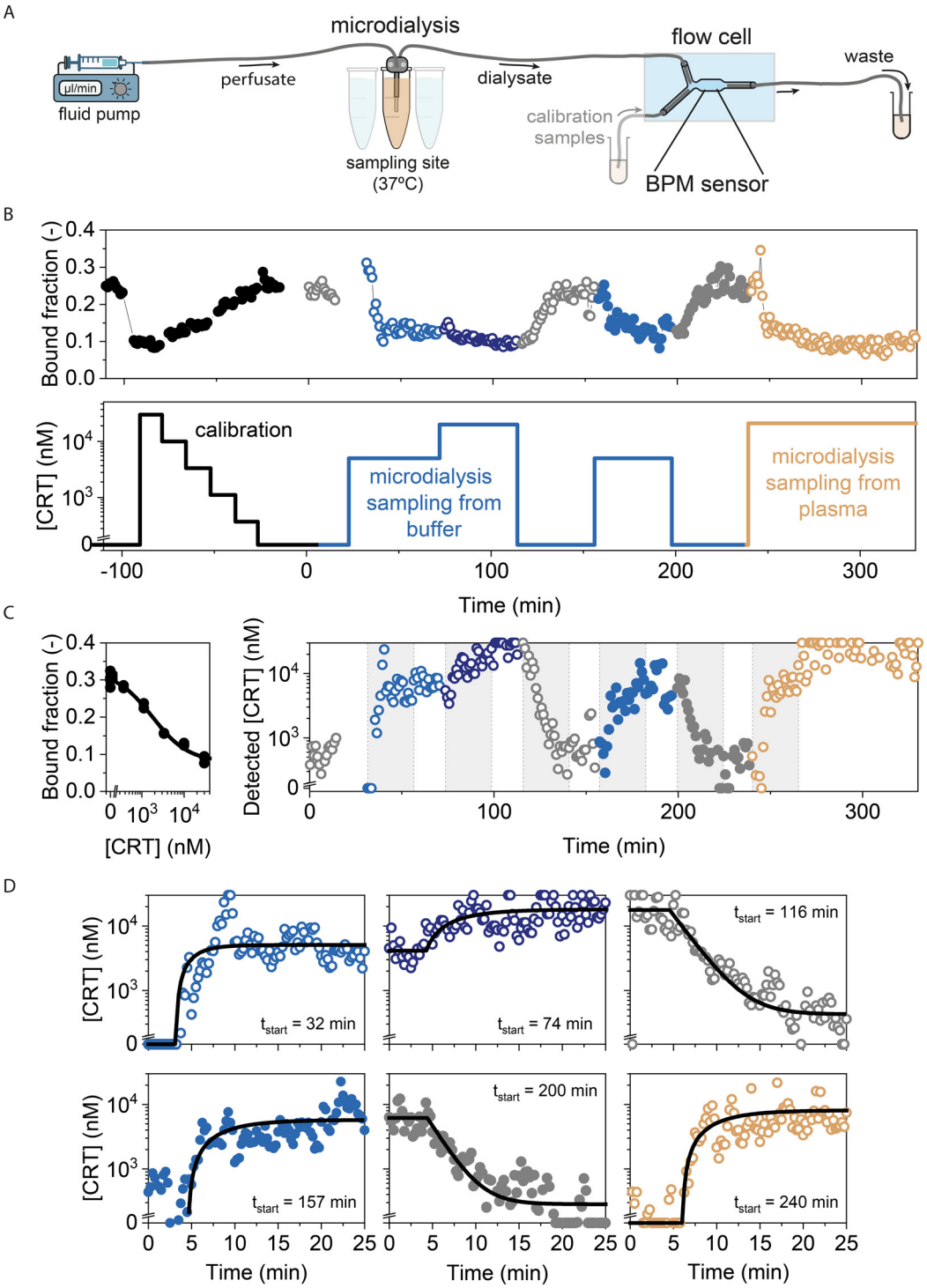

Fig. 5 Real-time cortisol monitoring with an integrated microdialysis-BPM system using a microdialysis probe with a 30 mm membrane length and a flowrate of 2 µl min^{-1}, with PBS plus 0.5 M NaCl as perfusate, and sampling from buffer (PBS with 0.5 M NaCl) and plasma (human blood plasma with 0.5 M NaCl). In all fluids, the NaCl was added for stability of the immunosensor.[24] A) Schematic drawing of the experimental system using microdialysis sampling from a series of fluid containers. The BPM flow cell has two inlets: one connected to the microdialysis probe and another one for the supply of calibration samples. The outlet of the flow cell is used for the collection of waste fluid or to draw calibration fluid into the flow cell with a syringe pump. B) Applied cortisol concentrations as a function of time (bottom panel) and measured sensor signal as a function of time (top panel). The first ~100 min were used for measuring calibration samples and thereafter microdialysis sampling from buffer and plasma was studied. Measurement blocks were manually started, automatically ended, and manually re-started, which sometimes caused gaps in the data series. C) Left panel: calibration curve, based on the black data points in panel B. Right panel: apparent cortisol concentrations as a function of time, based on the calibration curve and the signals measured in panel B ($t > 0$). D) Six sections are shown, corresponding to the shaded areas in panel C. The symbols correspond to the symbols in B and C. Data are fitted with single-exponential relaxation curves (black lines) of which the parameter values are provided in Table S5.† The long tails of relaxation curves for decreasing concentration steps are caused by the logarithmic *y*-axis scale.

the concentration change. These timescales should be suited for monitoring physiological cortisol dynamics as these occur on timescales in the order of tens of minutes up to hours.[19,28]

Further studies will focus on analytical aspects such as precision, calibrations, and accuracy, and how these depend on the microdialysis perfusion rate. Buffer compositions will be investigated, as these can affect microdialysis performance (*e.g.* osmotic pressure with respect to the biological medium) as well as sensor performance. It will be interesting to comparatively study microdialysis integration with other sensors for continuous biomolecular monitoring, such as continuous electrochemical aptamer-based sensors[29–31] and continuous fluorescence-based sensors.[32,33] Finally, tests in live biological systems of increasing complexity are an interesting next step to develop the technology toward future applications of continuous monitoring in (pre)clinical settings.

Experimental

Materials and methods

Materials. The oligonucleotides used in the study were purchased from Integrated DNA Technologies (IDT). Chemicals used in the study were purchased from Sigma, unless stated otherwise. Custom-made flow cell stickers (Custom 4 Well Secure Seal) were obtained from Grace Biolabs (USA) based on the dimensions as provided in Fig. S8.† Porcine whole blood was provided by LifeTec Group. Azorubine stock was based on JO-LA red food colouring containing E122.

Preparation of cortisol-DNA conjugates. Cortisol 3-CMO-NHS ester (Sigma-Aldrich, H6635) was coupled to ssDNA with a 5′ amine (amine – 5′-TGG TCT TAC CCC TGC CGC AC-3′), based on Li, Y. *et al.*,[34] with use of HOBt as described by Yan, J. *et al.*[22] To obtain cortisol–DNA conjugates, 45 μL of 60 Cortisol 3-CMO-NHS ester was mixed with 4 μL of 60 mM HOBt (Sigma-Aldrich; 54 802), 4 μL of 300 mM EDC (Sigma-Aldrich; E6383), and 4 μL of DIPEA (Sigma-Aldrich; 387649) in dimethylsulfoxide (DMSO). The reaction mixture was incubated at room temperature for 15 min.

Amine-modified DNA was diluted to 10 μM in MOPS buffer (50 mM MOPS (Sigma-Aldrich; M1254) and 0.5 M NaCl, pH 8.0), of which 72 μL was added to the mixture and left to react for 16 h (room temperature, 850 rpm). A fresh reaction mixture of cortisol, HOBt, EDC, and DIPEA was prepared as before, incubated for 15 min, added to the amine–DNA mixture and left to react for 6 h. The reaction was quenched by adding 25 μL of 500 mM NH_4OAc (Sigma-Aldrich; A1542).

The reaction mixture containing cortisol–DNA was dissolved in 0.15 mM NaCl in 98% ethanol, stored at −20 °C for 16 h, followed by spinning down at 17 000 g for 15 min at 4 °C. The pellet was washed a second time (0.15 mM NaCl in 98% ethanol), incubated at −20 °C for 75 min, centrifuged, and washed with 70% ethanol. After incubation at −20 °C for 75 min, it was centrifuged, and the cortisol–DNA was obtained after lyophilization. The cortisol–DNA was dissolved to 25 μM and the conjugation verified using gel electrophoresis with a 15% urea gel at 150 V for 90 minutes.

Cortisol preparation. Cortisol stock was prepared by dissolving 1 mg ml^{-1} in methanol (technical grade) and diluted further in either 0.5 M NaCl/PBS, 4–40% BSA in PBS, in human plasma (P9523-5 ml), or porcine plasma, or full porcine blood (supplied by LifeTec Group).

Plasma preparation. Human plasma (Sigma P9523-5 ml) was reconstituted using 5 ml MilliQ. Porcine plasma was prepared by taking the supernatant after centrifuging porcine blood (supplied by LifeTec Group) with 2000 × *g* at 4 °C for 15 minutes.

Biotinylation of antibody. The C53 antibody (Thermo Fisher Scientific, 2 mg mL^{-1}) was first buffer exchanged to PBS with Zeba Spin Desalting Columns, 7 k MWCO (89882, Thermo Fisher Scientific) according to manufacturer's instruction. EZ-Link NHS-PEG4-biotin was dissolved in DMSO at a final concentration of 4 mM. Then, 20-fold molar excess of NHS-PEG4-biotin was added to the antibodies and incubated at room temperature for 1 h. Excess NHS-PEG4-biotin was removed by Zeba Spin Desalting Columns, 7 k MWCO (89882, Thermo Fisher Scientific), and the biotinylated antibodies were stored in PBS with 0.1% bovine serum albumin (BSA) at a concentration of 1 μM.

Functionalization of BPM slides (PLL-g-PEG/azide). Plastic slides (Ibidi; 25 mm × 75 mm) were cleaned by 10 minutes of sonication in milliQ water and then dried with a nitrogen stream. After that, the slides were exposed to UV-ozone treatment for 30 minutes, followed by the attachment of a custom-made flow cell sticker (Grace Biolabs). The flow cell was filled with 20 μL 0.45 mg mL^{-1} poly(L-lysine)-grafted poly(ethylene glycol) (PLL(20)-g[3.5]-PEG(2), SuSoS) and 0.05 mg mL^{-1} azide functionalized PLL-g-PEG (PLL(15)-g[3.5]-PEG(2)-N3, Nanosoft Biotechnology LLC) as described by Lin *et al.*[34] 20 μl 0.5 nM of 221 bp dsDNA tether (221 bp dsDNA with biotin on one side and DBCO on the other), diluted in 0.5 M NaCl/PBS, was incubated for approximately 15 hours, followed by an incubation with 20 μl of 2 μM ssDNA-DBCO (DBCO – 5′-GTG CGG CAG GGG TAA GAC CA-3′) for at least 48 hours (RT, up to several months).

Functionalization of particles. Streptavidin-coated magnetic particles (10 mg mL^{-1}, Dynabeads MyOne Streptavidin C1, 65 001, Thermo Scientific) were incubated for 30 minutes within equal volume of 250 nM biotinylated cortisol antibodies with a total volume of 4 μl, on a rotating fin. Subsequently, 1.5 μl of 10 μM polyT-biotin (biotin – 5′-TTT TTT TTT TTT TTT T-3′) was added and incubated for 30 minutes on a rotating fin. The particle mixture was washed twice with 500 μl of 0.05% Tween20 in PBS, and then the particles were reconstituted in 300 μl of 0.5 M NaCl/PBS using magnetic separation. Finally, the particle mixture was sonicated in a sonication bath for 30 seconds to avoid particle aggregation.

Sensor assembly and cortisol detection. On the day of use, 250 μl of functionalized particles was injected

(Harvard pump 11 Elite, 40 μl min^{-1} withdrawal speed) into the flow cell (Grace BioLabs). Particles were incubated for 5 minutes, to allow particles to sediment to the substrate and attach to the DNA tethers. Thereafter, the slide was turned over to allow untethered particles to sediment away from the functionalized surface. Secondly, 400 μl of 100 μM of 1 kDa mPEG-biotin (PG1-BN-1 k, Nanocs) was added, which was incubated for 30 minutes. During incubation, the tethered particles were measured to determine the background signal. Activation of the system was done by adding 200 μl of 700 pM and 1 nM cortisol-DNA (analogue) and incubated for 20 minutes. Excess analogue was removed by washing the flow cell with 200 μl of 0.5 M NaCl/PBS, after which the media containing varying cortisol concentrations were added, with 200 μl for each sample. Particle motion was recorded for at least 10 minutes under flow by addition of ~25 μl calibration sample with a flowrate of 2 μl min^{-1}. Reported time in Fig. 5 and S9† is the time difference between each completed particle tracking period relative to the time of the first measured sample.

Cortisol detection with UV-vis spectroscopy. Analysis on a NanoDrop2000 was done on the same day as microdialysis sampling by loading 2 μl sample and read-out of the absorbance at 247 nm.

Microdialysis. A microdialysis probe (CMA/20, 20 kDa MWCO, 4 mm or 30 mm membrane length) was placed in a container with sample medium heated to 37 °C. A syringe pump (Harvard Pico Elite) was used to continuously infuse buffer with a rate of 0.5, 1.0, or 2.0 μl min^{-1}. A 10 ml syringe (airtight) was filled with PBS or 4% BSA as perfusate (spiked with cortisol for retro-dialysis and containing 0.5 M NaCl for BPM experiments). Intermittent sampling was done by placing the microdialysis outlet tubing in 200 μl PCR-tubes (VWR). Sample weight was determined by weighing the collection vials before and after sampling using an Analytical Balance (PCE-ABT 220).

Flow cell connections. Connections with flexible tubing (mono-lumen tubing, Freudenberg Medical, inner diameter of 0.76 mm) were made by placing a gel-loading pipette tip in the openings of the flow cell sticker and the tips were fixated using UV-glue (142-M Medical Device Adhesive & Coatings, DYMAX). The gel-loading tip was cut and flexible tubing with an inner diameter of 0.76 mm was shifted over the tip, creating a leak-free connection. The microdialysis outlet tubing (transparent) was connected by inserting the tubing into the side opening of the flow cell sticker and fixated using UV-glue. The microdialysis inlet tubing (blue) was connected to a blunt needle (Harvard 433243, cat # 72-5440) using a microdialysis Tubing adapter (red, Aurora Borealis Control BVP) that was placed in 100% ethanol for >2 minutes before putting over the tubing and needle. Perfusate was infused with at 10 ml air-tide syringe (VWR) using a syringe pump (Harvard Pico Elite).

Image recording and data analysis of BPM. Tethered particles were tracked before, during, and after analogue binding, and after each concentration change, on a Leica Microscope (DMI5000 M with a CTR6000 light source), at a total magnification of 10× using a high-speed FLIR CMOS camera (Point Grey Research Grashopper3 GS3-U3-23S6M-C, 1920 × 1200, pixel format: 8 raw, gain 10). The particle motion in a field of view of 1129 × 706 μm was recorded for at least 10 min at a frame rate of 30 Hz with 5 ms exposure time under dark-field illumination conditions with real-time particle tracking software as described by Bergkamp *et al.*[35] The localization of particles, analysis of particle motion and detection of switching events were done using phasor-based localization[36] and Maximum-likelihood Multiple-windows Change Point Detection method (MM-CPD).[35] The sensor response was corrected for drift over time using the method as described by Vu *et al.*[37]

Image recording and data analysis of azorubine. Glass slides (25 × 75 mm) were functionalized with a custom-made 12 μl flow cell sticker and connected to flexible tubing and the microdialysis probe, similar as described for BPM experiments. Azorubine was detected on a Leica Microscope (DM6000 B), at a total magnification of 2.5× using a high-speed FLIR CMOS camera (Point Grey Research Grashopper3 GS3-U3-32S4M-C, 1536 × 2048, pixel format: 8 raw, gain 0). The flow cell top and bottom edges were visible in a field of view of 2120 × 2828 μm and the intensity was recorded under bright-field illumination conditions with FlyCap2 software. Analysis of intensities was done using MATLAB.

SDS-PAGE gel electrophoresis. 4–20% Tris-Glycine gel (15 well; Fisher Scientific) was loaded with 15 μl of sample mixed with loading buffer, and 5 μl of Protein Standard (#1610373, Biorad). Gel electrophoresis was performed under 150 volt for 75 minutes. Gel was washed with MilliQ and subsequently incubated for 15 minutes with Coomassie Brilliant Blue R-250 Staining Solution (#1610436, Biorad). Destaining was done overnight in MilliQ.

Equations. Concentration-time profiles were fitted with a single-exponential relaxation function with a time delay, according to: $y = \begin{cases} y_{start}, \text{ for } t < t_0 \\ y_{start} + \Delta y \cdot \left(1 - \exp\left(-\frac{(t-t_0)}{\tau}\right)\right), \text{ for } t \geq t_0, \end{cases}$ with y_{start} equal to the starting level, Δy the amplitude of the signal change, t the time, t_0 the time delay, and τ the characteristic single-exponential relaxation time. This equation is available in Origin2020 under the name: ExpAssocDelay1, where the maximum number of iterations was set to 500. The sigmoidal fit of the dose-response curve was fitted with the equation: $S = S_{start} + (S_{end} - S_{start}) \cdot \frac{[CRT]}{EC50 + [CRT]}$, with S the signal, [CRT] the cortisol concentration, and EC50 the concentration of 50% effect. The microdialysis membrane areas were estimated based on the sum $A = A_1 + A_2$ of the area of a semi-sphere ($A_1 = \pi \cdot r^2$) and the area of a tube ($A_2 = 2 \cdot \pi \cdot r \cdot h$) with r = 0.25 mm and h = 4 or 30 mm. K_0 was calculated by dividing the fitted values ($K_0 \cdot A$) by the estimated membrane area.

Abbreviations

BPM	Biosensing by Particle Motion
CRT	Cortisol
MWCO	Molecular weight cut-off
Azo	Azorubine
BSA	Bovine Serum Albumin
ROI	Region of interest
FOV	Field of view

Author contributions

L. v. S. designed, performed, and analysed the experiments. All authors discussed results, interpreted data, and co-wrote the paper. All authors approved the submitted version of the manuscript.

Conflicts of interest

The authors declare the following competing financial interest(s): M. W. J. P. is listed as inventor on patent application WO/2016/096901 (Biosensor based on a tethered particle). M. W. J. P. is founder of Helia Biomonitoring BV that has a license to this patent. All authors declare no further competing interests.

Acknowledgements

We thank Sebastian Cajigas Bastidas for the functionalization of the BPM slides and particles. We thank Maud Linssen for assisting with the microdialysis sampling from whole blood and running of the SDS-PAGE gel. We thank Alissa Buskermolen for her contribution to the design of Fig. S11.† Part of this work was funded by the Dutch Research Council (NWO), section Applied and Engineering Sciences, under grant number 16255. Part of this work was funded by the Safe-N-Medtech H2020 project under grant agreement no. 814607.

References

1 U. Ungerstedt and C. Pyock, Functional correlates of dopamine neurotransmission, *Bull. Schweiz. Akad. Med. Wiss.*, 1974, **30**, 44–55.
2 U. Ungerstedt, M. Herrera-Marschitz, U. Jungnelius, L. Stahle, U. Tossman and T. Zetterström, Dopamine Synaptic Mechanisms Reflected in Studies Combining Behavioural Recordings and Brain Dialysis, *Advances in Dopamine Research*, 1982, pp. 219–231.
3 V. I. Chefer, A. C. Thompson, A. Zapata and T. S. Shippenberg, Overview of brain microdialysis, *Curr. Protoc. Neurosci.*, 2009, 1–35.
4 K. J. Hersini, L. Melgaard, P. Gazerani and L. J. Petersen, Microdialysis of inflammatory mediators in the skin: A review, *Acta Derm.-Venereol.*, 2014, **94**, 501–511.
5 F. Erdo, Microdialysis Techniques In Pharmacokinetic and Biomarker Studies Past, Present and Future Directions A Review, *Clin. Exp. Pharmacol.*, 2015, **05**, 1–11.
6 F. A. Zeiler, E. P. Thelin, M. Czosnyka, P. J. Hutchinson, D. K. Menon and A. Helmy, Cerebrospinal fluid and microdialysis cytokines in severe traumatic brain injury: A scoping systematic review, *Front. Neurol.*, 2017, **8**, 1–27.
7 P. M. Bernardi, F. Barreto and T. Dalla Costa, Application of a LC–MS/MS method for evaluating lung penetration of tobramycin in rats by microdialysis, *J. Pharm. Biomed. Anal.*, 2017, **134**, 340–345.
8 H. Rea and B. Kirby, A review of cutaneous microdialysis of inflammatory dermatoses, *Acta Derm.-Venereol.*, 2019, **99**, 945–952.
9 K. Rydenfelt, R. Strand-Amundsen, R. Horneland, S. Hødnebø, G. Kjøsen, S. E. Pischke, T. I. Tønnessen and H. Haugaa, Microdialysis and CO2 sensors detect pancreatic ischemia in a porcine model, *PLoS One*, 2022, **17**, 1–14.
10 S. A. N. Gowers, K. Hamaoui, P. Cunnea, S. Anastasova, V. F. Curto, P. Vadgama, G. Z. Yang, V. Papalois, E. M. Drakakis, C. Fotopoulou, S. G. Weber and M. G. Boutelle, High temporal resolution delayed analysis of clinical microdialysate streams, *Analyst*, 2018, **143**, 715–724.
11 M. L. Rogers, D. Feuerstein, C. L. Leong, M. Takagaki, X. Niu, R. Graf and M. G. Boutelle, Continuous online microdialysis using microfluidic sensors: Dynamic neurometabolic changes during spreading depolarization, *ACS Chem. Neurosci.*, 2013, **4**, 799–807.
12 S. M. Gunawardhana and S. M. Lunte, Continuous monitoring of adenosine and its metabolites using microdialysis coupled to microchip electrophoresis with amperometric detection, *Anal. Methods*, 2018, **10**, 3737–3744.
13 F. C. Alimagham, D. Hutter, N. Marco-García, E. Gould, V. H. Highland, A. Huefner, S. Giorgi-Coll, M. J. Killen, A. P. Zakrzewska, S. R. Elliott, K. L. H. Carpenter, P. J. Hutchinson and T. Hutter, Cerebral Microdialysate Metabolite Monitoring using Mid-infrared Spectroscopy, *Anal. Chem.*, 2021, **93**, 11929–11936.
14 J. H. Leopold, R. T. M. van Hooijdonk, M. Boshuizen, T. Winters, L. D. Bos, A. Abu-Hanna, A. M. T. Hoek, J. C. Fischer, E. C. van Dongen-Lases and M. J. Schultz, Point and trend accuracy of a continuous intravenous microdialysis-based glucose-monitoring device in critically ill patients: a prospective study, *Ann. Intensive Care*, 2016, **6**, 1–7.
15 C. Joukhadar and M. Uller, Microdialysis Current Applications in Clinical Pharmacokinetic Studies and its Potential Role in the Future, *Clin. Pharmacokinet.*, 2005, **44**, 895–913.
16 N. Plock and C. Kloft, Microdialysis - Theoretical background and recent implementation in applied life-sciences, *Eur. J. Pharm. Sci.*, 2005, **25**, 1–24.
17 D. A. Vassiliadi, I. Ilias, M. Tzanela, N. Nikitas, M. Theodorakopoulou, P. Kopterides, N. Maniatis, A. Diamantakis, S. E. Orfanos, I. Perogamvros, A. Armaganidis, B. G. Keevil, S. Tsagarakis and I. Dimopoulou, Interstitial cortisol obtained by microdialysis in mechanically ventilated septic patients: Correlations with total and free serum cortisol, *J. Crit. Care*, 2013, **28**, 158–165.

18 D. P. Fudulu, G. D. Angelini, F. F. Papadopoulou, J. Evans, T. Walker-Smith, I. Kema, M. Van Faassen, S. Stoica, M. Caputo, S. Lightman and B. Gibbison, The Peacock study: Feasibility of the dynamic characterisation of the paediatric hypothalamic-pituitary-adrenal function during and after cardiac surgery, *BMC Cardiovasc. Disord.*, 2020, **20**, 1–8.

19 R. Bhake, G. M. Russell, Y. Kershaw, K. Stevens, F. Zaccardi, V. E. C. Warburton, A. C. E. Linthorst and S. L. Lightman, Continuous free cortisol profiles in healthy men: Validation of microdialysis method, *J. Clin. Endocrinol. Metab.*, 2020, **105**, E1749–E1761.

20 L. Van Smeden, A. Saris, K. Sergelen, A. M. De Jong, J. Yan and M. W. J. Prins, Reversible Immunosensor for the Continuous Monitoring of Cortisol in Blood Plasma Sampled with Microdialysis, *ACS Sens.*, 2022, **7**, 3041–3048.

21 R. M. Lubken, M. H. Bergkamp, A. M. de Jong and M. W. J. Prins, Sensing Methodology for the Rapid Monitoring of Biomolecules at Low Concentrations over Long Time Spans, *ACS Sens.*, 2021, **6**, 4471–4481.

22 J. Yan, L. Van Smeden, M. Merkx, P. Zijlstra and M. W. J. Prins, Continuous Small-Molecule Monitoring with a Digital Single-Particle Switch, *ACS Sens.*, 2020, **5**, 1168–1176.

23 A. D. Buskermolen, Y. T. Lin, L. van Smeden, R. B. van Haaften, J. Yan, K. Sergelen, A. M. de Jong and M. W. J. Prins, Continuous biomarker monitoring with single molecule resolution by measuring free particle motion, *Nat. Commun.*, 2022, **13**, 1–12.

24 M. H. Bergkamp, S. Cajigas, L. J. IJzendoorn and M. W. J. Prins, High-throughput single-molecule sensors: how can the signals be analyzed in real time for achieving real-time continuous biosensing, *ACS Sens.*, 2023, **8**, 2271–2281.

25 V. J. A. Schuck, I. Rinas and H. Derendorf, *In vitro* microdialysis sampling of docetaxel, *J. Pharm. Biomed. Anal.*, 2004, **36**, 807–813.

26 I. Jacobson, M. Sandberg and A. Hamberger, Mass transfer in brain dialysis devices–a new method for the estimation of extracellular amino acids concentration, *J. Neurosci. Methods*, 1985, **15**, 263–268.

27 J. Melin, Z. P. Parra-Guillen, N. Hartung, W. Huisinga, R. J. Ross, M. J. Whitaker and C. Kloft, Predicting Cortisol Exposure from Paediatric Hydrocortisone Formulation Using a Semi-Mechanistic Pharmacokinetic Model Established in Healthy Adults, *Clin. Pharmacokinet.*, 2018, **57**, 515–527.

28 R. M. Torrente-Rodríguez, J. Tu, Y. Yang, J. Min, M. Wang, Y. Song, Y. Yu, C. Xu, C. Ye, W. W. IsHak and W. Gao, Investigation of Cortisol Dynamics in Human Sweat Using a Graphene-Based Wireless mHealth System, *Matter*, 2020, **2**, 921–937.

29 B. S. Ferguson, D. A. Hoggarth, D. Maliniak, K. Ploense, R. J. White, N. Woodward, K. Hsieh, A. J. Bonham, M. Eisenstein, K. W. Plaxco and H. T. Soh, Real-time, aptamer-based tracking of circulating therapeutic agents in living animals, *Sci. Transl. Med.*, 2013, **5**, 1–21.

30 R. J. Schoukroun-Barnes, R. Lauren, F. C. Macazo, B. Gutierrez, J. Lottermoser, J. Liu and R. White, Structure-Switching Electrochemical Aptamer-Based Sensors, *Physiol. Behav.*, 2017, **176**, 139–148.

31 A. M. Downs and K. W. Plaxco, Real-Time, *in vivo* Molecular Monitoring Using Electrochemical Aptamer Based Sensors: Opportunities and Challenges, *ACS Sens.*, 2022, **7**, 2823–2832.

32 A. A. Hariri, A. P. Cartwright, C. Dory, Y. Gidi, S. Yee, K. Fu, K. Yang, D. Wu, I. A. P. Thompson, N. Maganzini, T. Feagin, B. E. Young, B. H. Afshar, M. Eisenstein, M. Digonnet, J. Vuckovic and H. T. Soh, Continuous optical detection of small-molecule analytes in complex biomatrices, *bioRxiv*, 2023, preprint, DOI: **10.1101/2023.03.03.531030**.

33 I. A. P. Thompson, J. Saunders, L. Zheng, A. A. Hariri, N. Maganzini, A. P. Cartwright, J. Pan, S. Yee, C. Dory, M. Eisenstein, J. Vuckovic and H. T. Soh, An antibody-based molecular switch for continuous small-molecule biosensing, *Sci. Adv.*, 2023, **9**(38), 1–12.

34 Y. T. Lin, R. Vermaas, J. Yan, A. M. De Jong and M. W. J. Prins, Click-Coupling to Electrostatically Grafted Polymers Greatly Improves the Stability of a Continuous Monitoring Sensor with Single-Molecule Resolution, *ACS Sens.*, 2021, **6**, 1980–1986.

35 M. H. Bergkamp, L. J. Van IJzendoorn and M. W. J. Prins, Real-Time detection of state transitions in stochastic signals from biological systems, *ACS Omega*, 2021, **6**, 17726–17733.

36 K. J. A. Martens, A. N. Bader, S. Baas, B. Rieger and J. Hohlbein, Phasor based single-molecule localization microscopy in 3D (pSMLM-3D): An algorithm for MHz localization rates using standard CPUs, *J. Chem. Phys.*, 2018, **148**, 1–6.

37 C. Vu, Y. T. Lin, S. R. R. Haenen, J. Marschall, A. Hummel, S. F. A. Wouters, J. M. H. Raats, A. M. De Jong, J. Yan and M. W. J. Prins, Real-Time Immunosensor for Small-Molecule Monitoring in Industrial Food Processes, *Anal. Chem.*, 2023, **95**, 7950–7959.